Supplement of Atmos. Chem. Phys., 16, 4511–4527, 2016
http://www.atmos-chem-phys.net/16/4511/2016/
doi:10.5194/acp-16-4511-2016-supplement

Supplement of

Molecular transformations of phenolic SOA during photochemical aging in the aqueous phase: competition among oligomerization, functionalization, and fragmentation

Lu Yu et al.

Correspondence to: Qi Zhang (dkwzhang@ucdavis.edu)

Section S1: **Nano-DESI measurement and data analysis**

The nano-DESI analyses were performed using a high-resolution LTQ-Orbitrap mass spectrometer (Thermo Electron, Bremen, Germany) with a resolving power (m/Δm) of 100,000 at *m/z* = 400. The instrument is equipped with a nano-DESI source assembled from two fused-silica capillaries (150 μm o.d./50 μm i.d.) (*Roach et al., 2010*). The analysis was performed under the following conditions: spray voltage of 3-5 kV, 0.5-1 mm distance from the tip of the nanospray capillary to the 250 ^{o}C heated inlet of the LTQ-Orbitrap, and 0.3-0.9 μL/min flow rate of acetonitrile : water (7:3 volume) solvent. Both positive and negative mode mass spectra were acquired using the Xcalibur software (Thermo Electron, Inc.).

Signals with S/N > 10 were picked out using the Decon2LS software developed at the Pacific Northwest National Laboratory (PNNL) (*Jaitly et al., 2009*). Data was further processed with Microsoft Excel using a set of built-in macros developed by Roach et al. (*2011*). The background and sample peaks were first aligned, and the peaks corresponding to ^{13}C isotopes were removed. Peaks in the sample spectra that are at least 10 times bigger than the corresponding peaks in the background spectra were retained for further analysis. Peaks were segregated into different groups using the higher-order mass defect transformation developed by Roach et al. (*2011*). Molecular formula was assigned with Formula Calculator v. 1.1 (http://www.magnet.fsu.edu/usershub/scientificdivisions/icr/icr_software.html) using the following constraints: C ≥ 0, H ≥ 0, O ≥ 0 for the negative ion mode data and C ≥ 0, H ≥ 0, O ≥ 0, Na ≤ 1 for the positive ion mode data. Approximately 70% of the peaks can be assigned with molecular formula within these constraints.

Section S2: **HR-AMS measurement and data analysis**

In this study, a High Resolution Time-of-Flight Aerosol Mass Spectrometer (Aerodyne Res. Inc., Billerica, MA; thereinafter referred to as AMS) was used to characterize the bulk chemical composition and elemental ratios of the low-volatility substances. The working principles of the AMS have been discussed previously (*DeCarlo et al., 2006;Canagaratna et al., 2007*). Briefly, the AMS analyzes nonrefractory aerosols that can be evaporated at ~ 600 °C via 70 eV EI mass spectrometry. In this study, the AMS was operated in "V" mode (mass resolutions of ~ 3000) to acquire mass spectra up to *m/z* 500.

The AMS data were analyzed using the AMS data analysis software (SQUIRREL v1.12 and PIKA v1.53 downloaded from http://cires.colorado.edu/jimenez-group/ToFAMSResources/ToFSoftware/). The V-mode data was analyzed to obtain high resolution mass spectra (HRMS), the atomic ratios of oxygen-to-carbon (O/C), hydrogen-to-carbon (H/C) and the organic mass-to-carbon ratio (OM/OC) (*Aiken et al., 2008*). The relative humidity measured at the AMS inlet was very low (< 2%), and we assume that contribution from gaseous water molecules was negligible. The H_2O^+ signal of organics was thus determined as the difference between the measured H_2O^+ signal and that produced by sulfates (*Allan et al., 2004*).

A solution composed of equal mass concentrations of ammonium sulfate and sucrose ($C_{12}H_{22}O_{11}$) was aatmozied and analyzed using AMS. The measured O/C and H/C ratio is 0.95 and 1.98 respectively. The error for O/C and H/C measurement is 3% and 8% respectively. Thus, the atomization procedure generates nearly equal amount of solutes in complex mixture.

Table S1 Most abundant compounds identified in SYR aqSOA formed during different stages of the •OH-mediated reactions.

No.	Molecular formula[a]	Proposed structure	C^* (μg m^{-3}) at 25 ◦C, 1 atm[b]	Relative abundance (ranking)[c]		
				P1: 0-2 hrs	P2: 2-4 hrs	P3: 4-6 hrs
1	$C_{16}H_{18}O_6$ (306.1103)	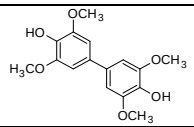	3.2E-03	100 (1)	14 (66)	0.0 (N/A)
2	$C_{15}H_{18}O_7$ (310.1052)	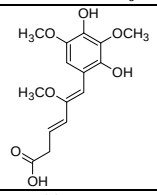	1.7E-05	56 (2)	100 (1)	27 (28)
3	$C_{15}H_{16}O_6$ (292.0946)	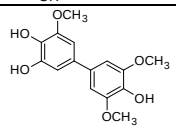	3.4E-04	46 (3)	8.6 (109)	0.4 (592)
4	$C_{15}H_{16}O_9$ (340.0794)	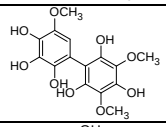	3.9E-12	28 (4)	93 (2)	100 (1)
5	$C_{13}H_{14}O_7$ (282.0739)	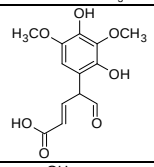	5.8E-08	19 (5)	48 (5)	29 (21)
6	$C_{15}H_{16}O_8$ (324.0845)	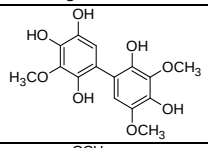	2.8E-09	19 (6)	23 (31)	15 (79)
7	$C_{16}H_{18}O_7$ (322.1052)	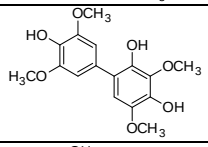	1.7E-05	18 (7)	3.7 (261)	0.7 (508)
8	$C_{14}H_{12}O_7$ (292.0583)	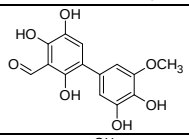	4.0E-11	17 (8)	39 (9)	11 (107)
9	$C_{15}H_{18}O_{10}$ (358.0900)	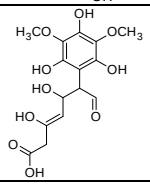	1.5E-13	13 (9)	50 (4)	49 (5)
10	$C_{14}H_{14}O_8$ (310.0688)	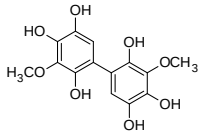	9.9E-11	12 (10)	45 (6)	42 (7)

11	$C_{12}H_{12}O_7$ (268.0583)	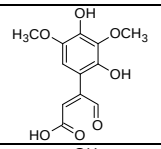	1.3E-07	11 (13)	43 (7)	37 (11)
12	$C_{13}H_{16}O_8$ (300.0845)	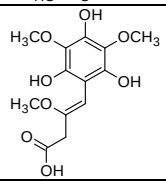	3.4E-07	8.1 (22)	39 (8)	38 (10)
13	$C_6H_8O_6$ (176.0321)	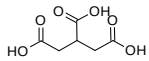	3.1E+04	7.2 (27)	56 (3)	80 (2)
14	$C_{14}H_{16}O_9$ (328.0794)	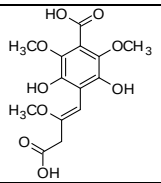	7.6E-11	6.7 (30)	31 (10)	40 (8)
15	$C_5H_6O_5$ (146.0215)	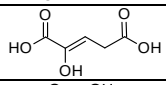	2.7E+01	4.6 (48)	30 (13)	42 (6)
16	$C_4H_6O_5$ (134.0215)	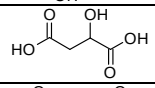	3.3E+00	4.4 (50)	24 (23)	61 (3)
17	$C_5H_6O_6$ (162.0164)	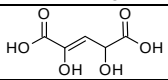	5.0E-02	4.2 (54)	30 (14)	50 (4)
18	$C_6H_6O_6$ (174.0164)	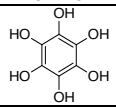	5.2E-05	3.4 (66)	24 (26)	40 (9)

[a] Molecular formulas and proposed structures of 18 compounds identified according to (-) nano-DESI spectra. They represent the top 10 most abundant aqSOA compounds observed at each reaction stage. The exact molecular weight of each compound is shown in parentheses.

[b] Estimated saturation concentrations (C^*, μg m^{-3}) of the compounds at 25 ◦C, 1 atm, determined using the Nannoolal vapor pressure and extrapolation method.

[c] Relative abundances (%) of the compounds and, in parentheses, their abundance ranks counted in the sorted relative abundance list of all the compounds identified in the nano-DESI mass spectrum of the specified time period.

Table S2 Most abundant compounds identified in GUA aqSOA formed during different stages of the $^{3}C^{*}$-mediated reactions.

No.	Molecular formula[a]	Proposed structure	C^{*} (μg m^{-3}) at 25 ◦C, 1 atm[b]	Relative abundance (ranking)[c]		
				P1: 0-2 hrs	P2: 2-4 hrs	P3: 4-6 hrs
1	$C_{14}H_{14}O_4$ (246.0892)	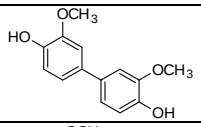	8.8E-01	100 (1)	60 (2)	32 (2)
2	$C_{14}H_{14}O_6$ (278.0790)	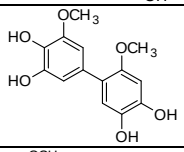	2.5E-05	79 (2)	100 (1)	100 (1)
3	$C_{21}H_{20}O_6$ (368.1259)	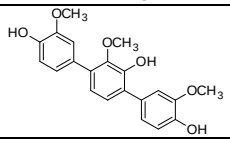	4.1E-11	65 (3)	34 (3)	16 (6)
4	$C_{20}H_{18}O_6$ (354.1103)	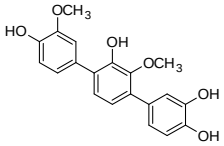	8.0E-09	28 (4)	23 (4)	12 (10)
5	$C_{13}H_{12}O_4$ (232.0735)	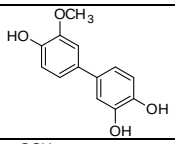	8.7E-02	19 (5)	15 (9)	11 (11)
6	$C_{21}H_{18}O_8$ (398.1001)	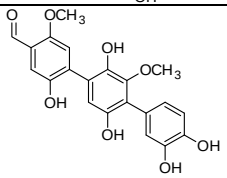	5.7E-14	16 (6)	22 (5)	20 (3)
7	$C_{21}H_{20}O_8$ (400.1158)	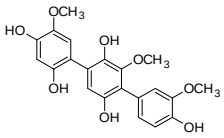	5.0E-13	14 (7)	19 (6)	18 (4)
8	$C_{14}H_{12}O_6$ (276.0634)	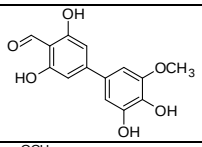	3.1E-06	13 (8)	17 (7)	17 (5)
9	$C_{28}H_{26}O_8$ (490.1627)	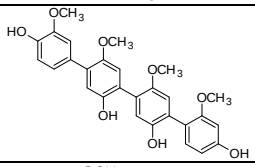	1.8E-15	10 (9)	4.3 (23)	1.3 (104)
10	$C_{14}H_{14}O_5$ (262.0841)	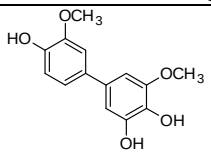	6.0E-03	9.2 (10)	7.0 (12)	4.7 (23)

11	$C_{20}H_{16}O_7$ (368.0896)	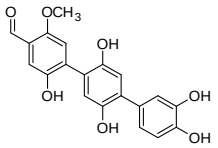	1.6E-12	9.0 (11)	16 (8)	14 (8)
12	$C_{13}H_{10}O_5$ (246.0528)	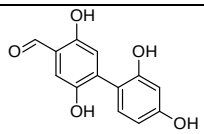	4.7E-05	6.9 (12)	13 (10)	15 (7)
13	$C_{13}H_{12}O_6$ (264.0634)	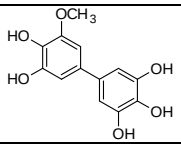	1.1E-06	6.2 (14)	11 (11)	14 (9)

[a] Molecular formulas and proposed structures of 13 compounds identified according to (-) nano-DESI spectra. They represent the top 10 most abundant aqSOA compounds observed at each reaction stage. The exact molecular weight of each compound is shown in parentheses.

[b] Estimated saturation concentrations (C^*, μg m^{-3}) of the compounds at 25 ◦C, 1 atm, determined using the Nannoolal vapor pressure and extrapolation method.

[c] Relative abundances (%) of the compounds and, in parentheses, their abundance ranks counted in the sorted relative abundance list of all the compounds identified in the nano-DESI mass spectrum of the specified time period.

Table S3 Most abundant compounds identified in GUA aqSOA formed during different stages of the •OH-mediated reactions.

No.	Molecular formula[a]	Proposed structure	C^* (μg m^{-3}) at 25 ◦C, 1 atm[b]	Relative abundance (ranking)[c]		
				P1: 0-2 hrs	P2: 2-4 hrs	P3: 4-6 hrs
1	$C_{14}H_{14}O_6$ (278.0790)	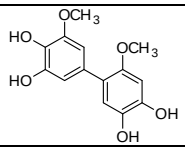	2.5E-05	100 (1)	100 (1)	100 (1)
2	$C_{14}H_{14}O_4$ (246.0892)	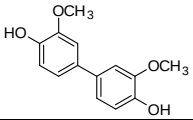	8.8E-01	52 (2)	37 (2)	18 (3)
3	$C_{21}H_{20}O_6$ (368.1259)	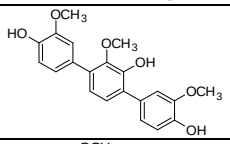	4.1E-11	28 (3)	10 (7)	5.1 (21)
4	$C_{13}H_{12}O_4$ (232.0735)	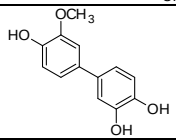	8.7E-02	23 (4)	15 (5)	12 (8)
5	$C_{20}H_{18}O_6$ (354.1103)	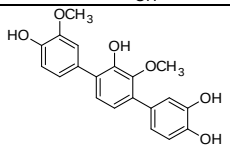	8.0E-09	19 (5)	8.1 (11)	4.9 (22)
6	$C_8H_6O_3$ (150.0317)	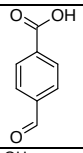	5.2E+02	15 (6)	0.0 (N/A)	1.7 (82)
7	$C_{14}H_{12}O_6$ (276.0634)	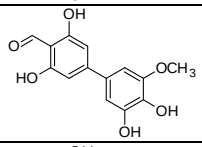	3.1E-06	13 (7)	17 (3)	17 (4)
8	$C_{13}H_{10}O_5$ (246.0528)	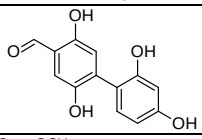	4.7E-05	12 (8)	15 (4)	18 (2)
9	$C_{21}H_{18}O_8$ (398.1001)	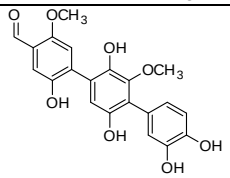	5.7E-14	9.9 (9)	8.7 (10)	8.3 (12)
10	$C_{13}H_{12}O_6$ (264.0634)	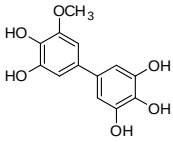	1.1E-06	9.7 (10)	12 (6)	16 (5)

11	$C_{13}H_{10}O_4$ (230.0579)	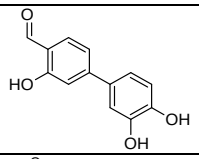	1.2E-02	6.2 (16)	9.4 (9)	14 (6)
12	$C_{13}H_{10}O_3$ (214.0630)	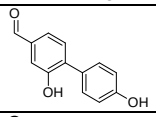	2.0E+00	5.5 (19)	6.7 (14)	8.7 (10)
13	$C_7H_{10}O_6$ (190.0477)	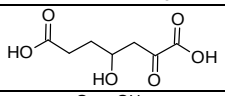	4.4E-03	3.7 (21)	10 (8)	13 (7)
14	$C_4H_6O_5$ (134.0215)	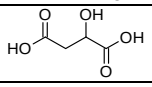	5.6E+00	0.0 (N/A)	0.0 (N/A)	9.6 (9)

[a] Molecular formulas and proposed structures of 14 compounds identified according to (-) nano-DESI spectra. They represent the top 10 most abundant aqSOA compounds observed at each reaction stage. The exact molecular weight of each compound is shown in parentheses.

[b] Estimated saturation concentrations (C^*, μg m^{-3}) of the compounds at 25 ◦C, 1 atm, determined using the Nannoolal vapor pressure and extrapolation method.

[c] Relative abundances (%) of the compounds and, in parentheses, their abundance ranks counted in the sorted relative abundance list of all the compounds identified in the nano-DESI mass spectrum of the specified time period.

Table S4 Most abundant compounds identified in PhOH aqSOA formed during different stages of the $^3C^*$-mediated reactions.

No.	Molecular formula[a]	Proposed structure	C^* (μg m^{-3}) at 25 °C, 1 atm[b]	Relative abundance (ranking)[c]		
				P1: 0-5 hrs	P2: 5-9 hrs	P3:19-20 hrs
1	$C_{12}H_{10}O_3$ (202.0630)	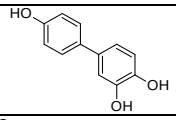	9.0E-01	100 (1)	100 (1)	5.7 (18)
2	$C_{18}H_{14}O_3$ (278.9042)	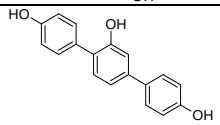	6.5E-04	88 (2)	41 (7)	0.5 (194)
3	$C_{18}H_{14}O_4$ (294.0892)	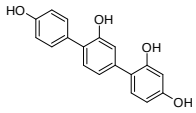	2.4E-06	45 (3)	40 (8)	1.9 (69)
4	$C_{12}H_{10}O_2$ (186.0680)	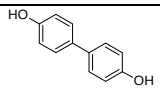	9.2E+01	27 (4)	25 (10)	0.6 (175)
5	$C_{13}H_{10}O_3$ (214.0630)	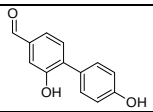	2.0E+00	21 (5)	42 (5)	23 (5)
6	$C_{18}H_{12}O_5$ (308.0684)	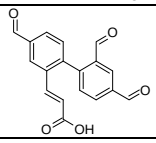	4.0E-07	21 (6)	44 (4)	1.8 (80)
7	$C_{20}H_{14}O_6$ (350.0790)	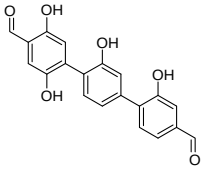	1.1E-10	20 (7)	70 (2)	26 (4)
8	$C_{24}H_{18}O_4$ (370.1204)	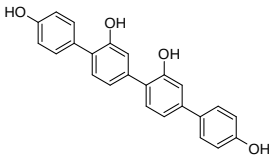	9.2E-10	16 (8)	5.9 (45)	0.0 (N/A)
9	$C_{13}H_{10}O_4$ (230.0579)	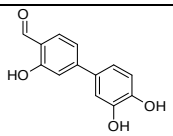	1.2E-02	16 (9)	42 (6)	34 (2)
10	$C_{18}H_{12}O_4$ (292.0735)	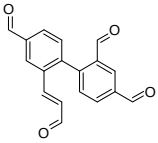	6.0E-04	13 (10)	8.9 (23)	0.1 (377)
11	$C_{14}H_{10}O_5$ (258.0528)	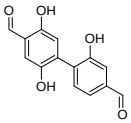	1.0E-04	11 (11)	31 (9)	17 (9)

12	$C_8H_6O_5$ (182.0215)		8.8E-02	5.3 (18)	9.4 (21)	8.8 (10)
13	$C_7H_6O_3$ (138.0317)		9.3E+03	4.2 (21)	17 (11)	20 (6)
14	$C_7H_6O_4$ (154.0266)		1.6E+01	2.4 (37)	9.6 (20)	19 (7)
15	$C_4H_4O_4$ (116.0110)		1.1E+03	0.6 (95)	6.5 (37)	18 (8)
16	$C_4H_6O_5$ (134.0215)		5.6E+00	0.0 (N/A)	52 (3)	100 (1)
17	$C_4H_6O_4$ (118.0266)		2.3E+03	0.0 (N/A)	0.0 (N/A)	34 (3)

[a] Molecular formulas and proposed structures of 17 compounds identified according to (-) nano-DESI spectra. They represent the top 10 most abundant aqSOA compounds observed at each reaction stage. The exact molecular weight of each compound is shown in parentheses.

[b] Estimated saturation concentrations (C^*, μg m^{-3}) of the compounds at 25 ◦C, 1 atm, determined using the Nannoolal vapor pressure and extrapolation method.

[c] Relative abundances (%) of the compounds and, in parentheses, their abundance ranks counted in the sorted relative abundance list of all the compounds identified in the nano-DESI mass spectrum of the specified time period.

Table S5 Most abundant compounds identified in PhOH aqSOA formed at different stages of the •OH-mediated reactions.

No.	Molecular formula[a]	Proposed structure	C^* (μg m^{-3}) at 25 ◦C, 1 atm[b]	Relative abundance (ranking)[c]		
				P1: 0-6 hrs	P2: 6-12 hrs	P3: 23-24 hrs
1	$C_{13}H_{10}O_4$ (230.0579)	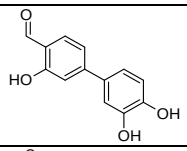	1.2E-02	100 (1)	100 (1)	48 (2)
2	$C_{13}H_{10}O_3$ (214.0630)	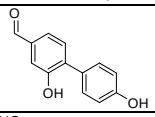	2.0E+00	90 (2)	60 (4)	19 (9)
3	$C_{12}H_{10}O_3$ (202.0630)	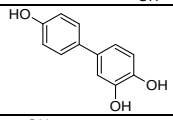	9.0E-01	48 (3)	24 (8)	2.1 (86)
4	$C_{20}H_{14}O_6$ (350.0790)	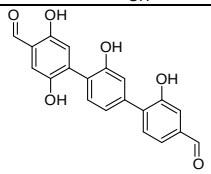	1.1E-10	47 (4)	68 (2)	29 (4)
5	$C_{14}H_{10}O_5$ (258.0528)	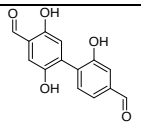	1.0E-04	39 (5)	34 (5)	15 (12)
6	$C_8H_6O_3$ (150.0317)	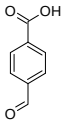	8.5E-08	27 (6)	7.3 (32)	2.0 (88)
7	$C_6H_6O_5$ (158.0215)	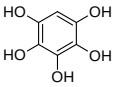	2.2E-02	19 (7)	27 (7)	19 (8)
8	$C_7H_6O_4$ (154.0266)	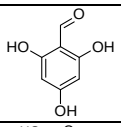	1.6E+01	15 (8)	27 (6)	26 (5)
9	$C_8H_6O_5$ (182.0215)	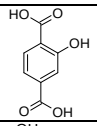	8.8E-02	15 (9)	11 (22)	7.4 (23)
10	$C_{12}H_{10}O_4$ (218.0579)	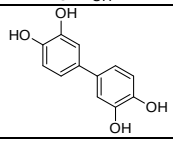	4.7E-03	14 (10)	19 (10)	4.5 (34)
11	$C_4H_6O_5$ (134.0215)	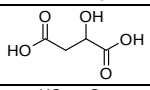	5.2E+00	0.0 (N/A)	62 (3)	100 (1)
12	$C_{11}H_{10}O_8$ (270.0376)	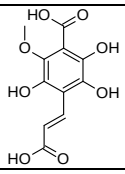	4.7E-11	0.0 (N/A)	20 (9)	10 (14)

13	$C_4H_6O_4$ (118.0266)		2.3E+03	0.0 (N/A)	0.0 (N/A)	33 (3)
14	$C_6H_8O_6$ (176.0321)		3.1E+04	9.0 (19)	16 (11)	21 (6)
15	$C_4H_4O_4$ (116.0110)		1.1E+03	1.6 (48)	12 (16)	21 (7)
16	$C_5H_6O_6$ (162.0164)		5.0E-02	1.8 (44)	7.1 (35)	16 (10)

[a] Molecular formulas and proposed structures of 16 compounds identified according to (-) nano-DESI spectra. They represent the top 10 most abundant aqSOA compounds observed at each reaction stage. The exact molecular weight of each compound is shown in parentheses.

[b] Estimated saturation concentrations (C^*, μg m^{-3}) of the compounds at 25 ◦C, 1 atm, determined using the Nannoolal vapor pressure and extrapolation method.

[c] Relative abundances (%) of the compounds and, in parentheses, their abundance ranks counted in the sorted relative abundance list of all the compounds identified in the nano-DESI mass spectrum of the specified time period.

Table S6 Most abundant compounds identified in SYR aqSOA formed at different stages of the $^{3}C^{*}$-mediated reactions using (+) nano-DESI MS.

No.	Molecular formula[a]	Proposed structure	C^{*} (μg m^{-3}) at 25 ◦C, 1 atm[b]	Relative abundance (%) (ranking)[c]		
				P1: 0-2 hrs	P2: 2-4 hrs	P3: 4-6 hrs
1	$C_{16}H_{18}O_6$ (306.1103)	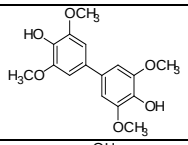	3.1E-03	100 (1)	0.0 (N/A)	0.0 (N/A)
2	$C_{15}H_{18}O_7$ (310.1052)	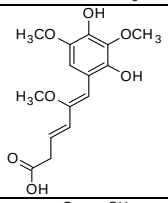	1.7E-05	78.1 (2)	30.9 (5)	0.5 (53)
3	$C_{10}H_8O_3$ (176.0473)	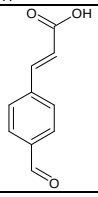	2.3E-09	43.2 (3)	100 (1)	100 (1)
4	$C_{12}H_{14}O_4$ (222.0892)	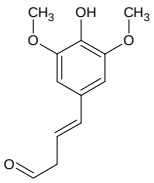	2.1E-09	18.7 (4)	31.9 (4)	43.7 (2)
5	$C_{14}H_{14}O_6$ (278.0790)	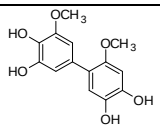	2.5E-05	14.5 (5)	4.7 (27)	1.1 (23)
6	$C_{13}H_{14}O_5$ (250.0841)	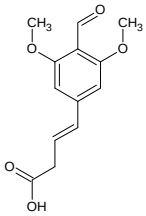	2.0E-12	8.7 (6)	2.2 (48)	0.2 (115)
7	$C_{13}H_{14}O_7$ (282.0740)	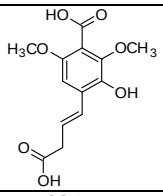	5.8E-08	7.2 (7)	14.0 (11)	2.7 (7)
8	$C_{16}H_{18}O_7$ (322.1053)	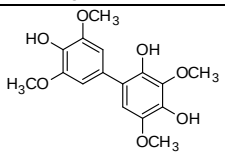	1.7E-05	6.2 (8)	0 (N/A)	0.0 (N/A)

9	$C_{15}H_{16}O_6$ (292.0946)		3.4E-04	5.3 (9)	0.0 (N/A)	0.0 (N/A)
10	$C_{15}H_{18}O_{10}$ (358.0900)		1.5E-13	4.8 (10)	64.5 (2)	5.0 (4)
11	$C_8H_{10}O_6$ (202.0477)		5.9E-02	4.5 (11)	49.7 (3)	5.3 (3)
12	$C_8H_{10}O_7$ (218.0427)		4.2E-02	0.8 (42)	25.1 (6)	0.6 (50)
13	$C_{15}H_{16}O_9$ (340.0794)		3.9E-12	3.9 (12)	23.0 (7)	3.1 (6)
14	$C_8H_4O_3$ (148.0160)		7.3E-06	0.0 (N/A)	22.5 (8)	3.5 (5)
15	$C_{15}H_{18}O_9$ (342.0950)		6.6E-21	2.3 (17)	21.5 (9)	1.0 (28)
16	$C_7H_{12}O_7$ (208.0583)		N/A	1.0 (33)	19.0 (10)	1.0 (27)
17	$C_{14}H_{16}O_{10}$ (344.0743)		2.7E-14	0.6 (46)	7.9 (14)	1.9 (8)
18	$C_{14}H_{16}O_9$ (328.0794)		7.6E-11	0.8 (39)	6.5 (20)	1.7 (9)

19	$C_{14}H_{16}O_8$ (312.0845)	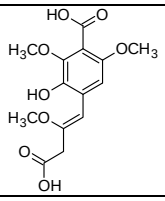	2.5E-08	0.9 (35)	6.2 (22)	1.5 (10)

[a] Molecular formulas and proposed structures of 19 compounds identified according to (+) nano-DESI spectra. They represent the top 10 most abundant aqSOA compounds observed at each reaction stage. The exact molecular weight of each compound is shown in parentheses.

[b] Estimated saturation concentrations (C^*, μg m^{-3}) of the compounds at 25 ◦C, 1 atm, determined using the Nannoolal vapor pressure and extrapolation method.

[c] Relative abundances (%) of the compounds and, in parentheses, their abundance ranks counted in the sorted relative abundance list of all the compounds identified in the nano-DESI mass spectrum of the specified time period.

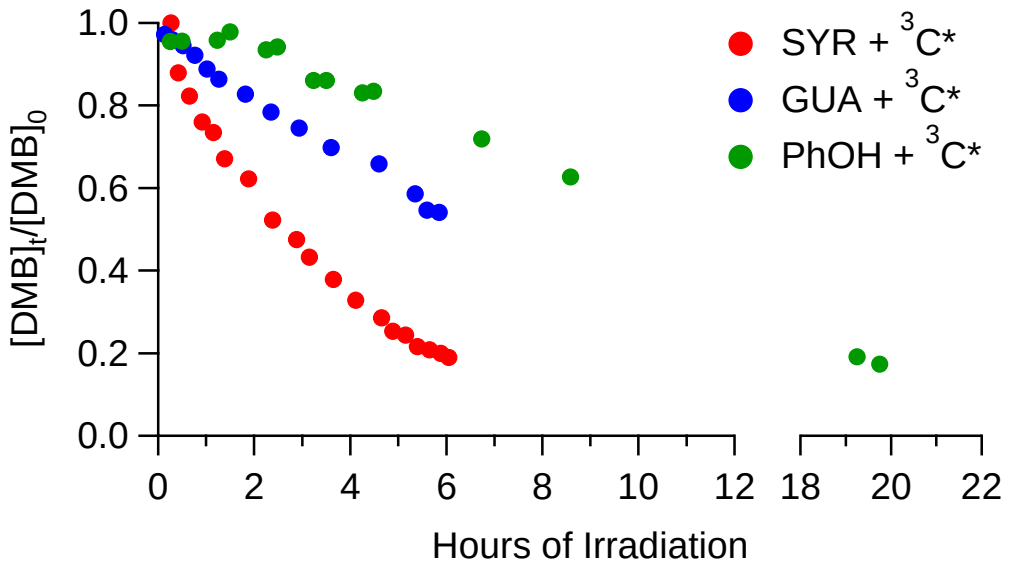

Figure S1. Evolution of concentrations of 3,4-DMB as a function of reaction time during individual experiments. Different reaction conditions are represented by corresponding colors.

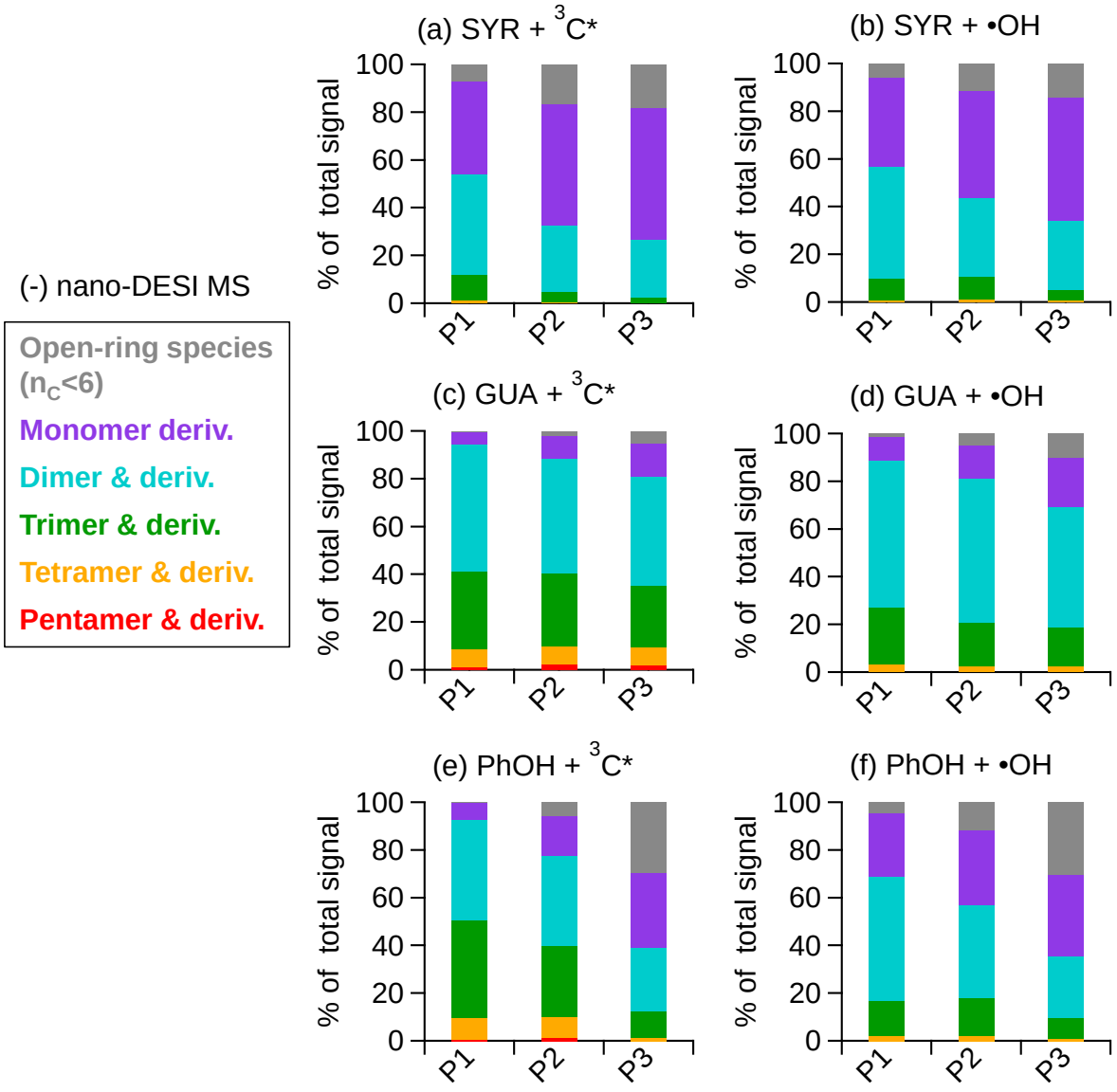

Figure S2. The signal-weighted distributions of **(a-b)** SYR, **(c-d)** GUA, and **(e-f)** PhOH aqSOA formed during three different stages of the ^{3}C*- and •OH-mediated reactions, respectively, based on the degree of oligomerization. The data are from the (–) nano-DESI MS spectra.

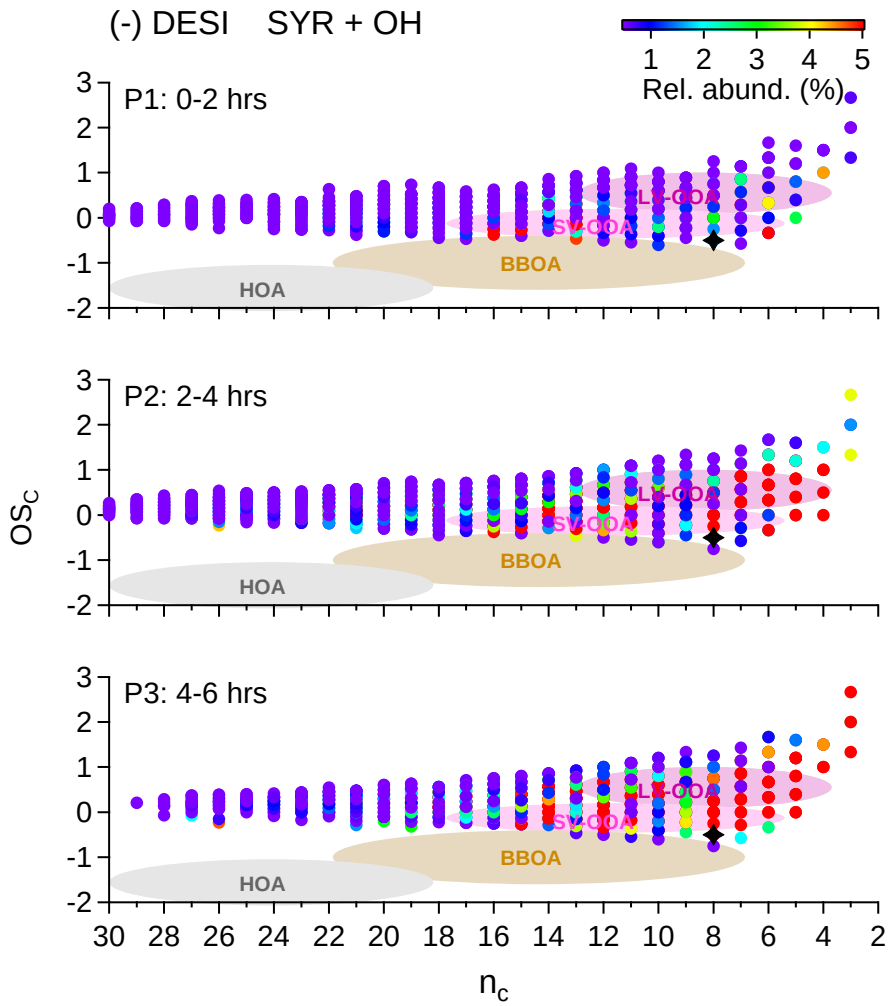

Figure S3. OS_C and n_C of SYR aqSOA formed during different stages of •OH-mediated reactions determined based on (-) nano-DESI MS spectra. Signals are colored by the relative abundance of the molecules. The black star at n_C = 8 represents SYR. The shaded ovals indicate locations of different ambient organic aerosol classes reported in Kroll et al. (*2011*).

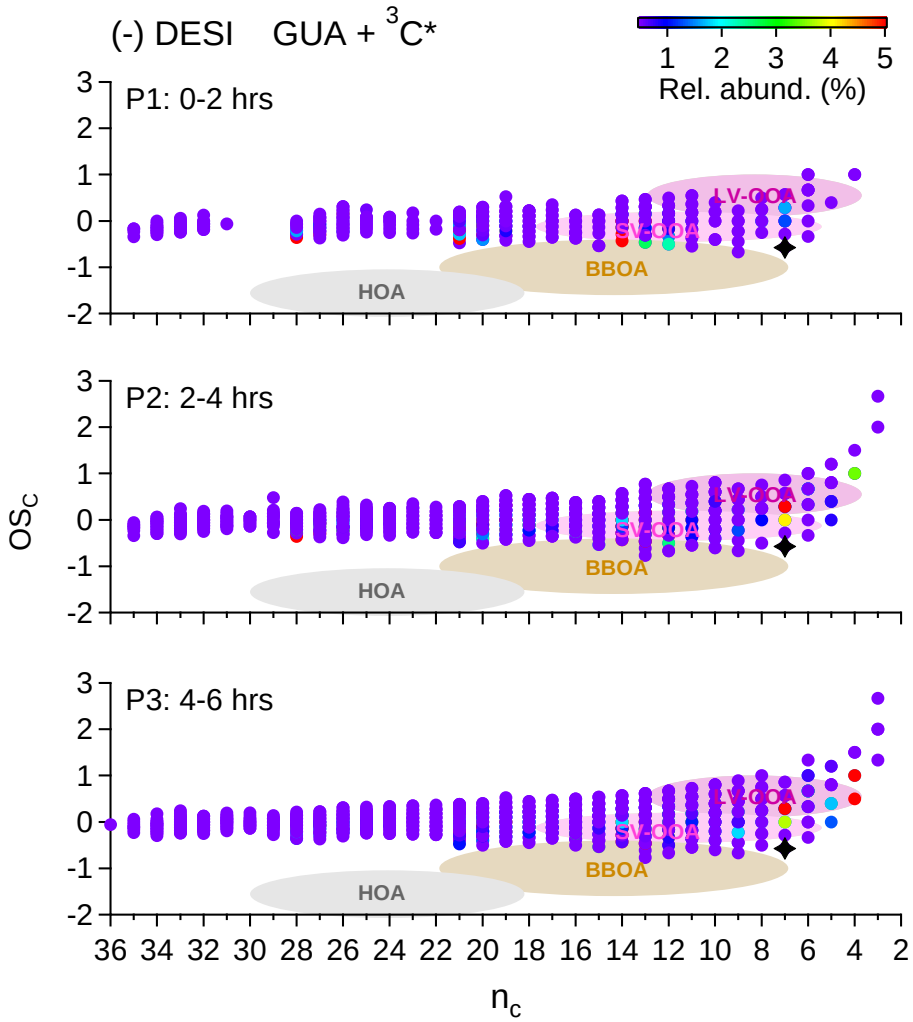

Figure S4. OS_C and n_C of GUA aqSOA formed during different stages of $^3C^*$-mediated reactions determined based on (-) nano-DESI MS spectra. Signals are colored by the relative abundance of the molecules. The black star at $n_C = 7$ represents GUA. The shaded ovals indicate locations of different ambient organic aerosol classes reported in Kroll et al. (*2011*).

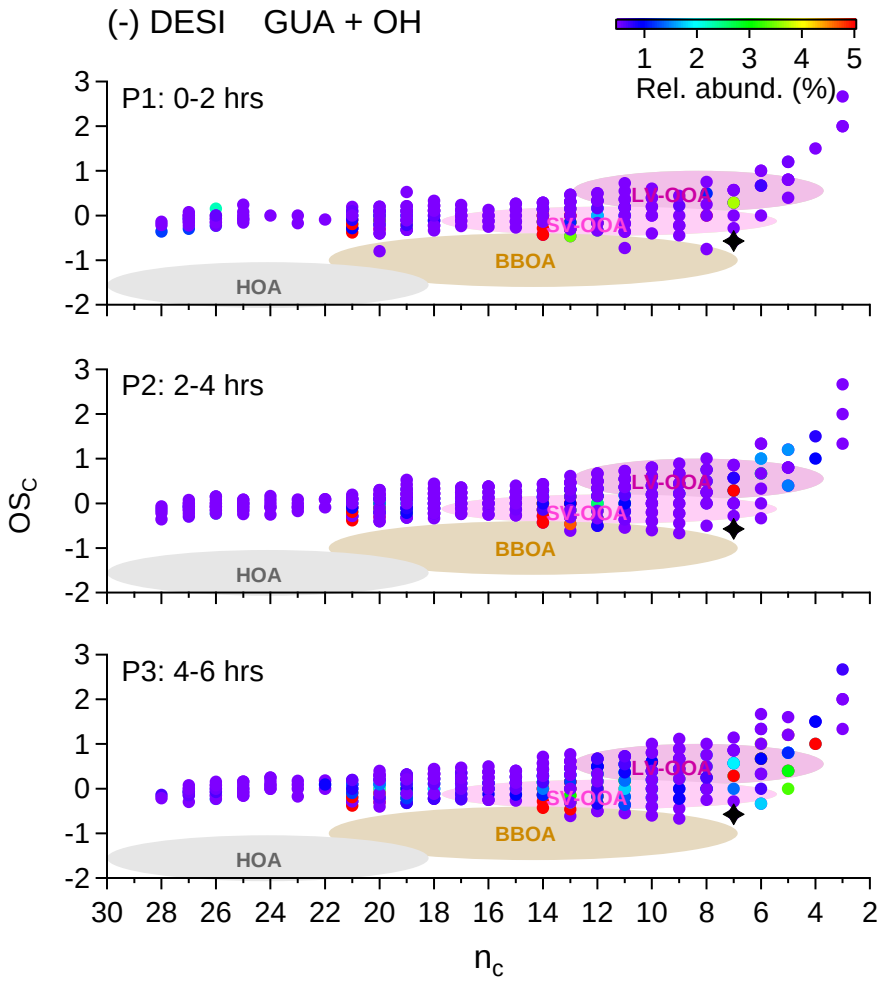

Figure S5. OS_C and n_C of GUA aqSOA formed during different stages of •OH-mediated reactions determined based on (-) nano-DESI MS spectra. Signals are colored by the relative abundance of the molecules. The black star at $n_C = 7$ represents GUA. The shaded ovals indicate locations of different ambient organic aerosol classes reported in Kroll et al. (*2011*).

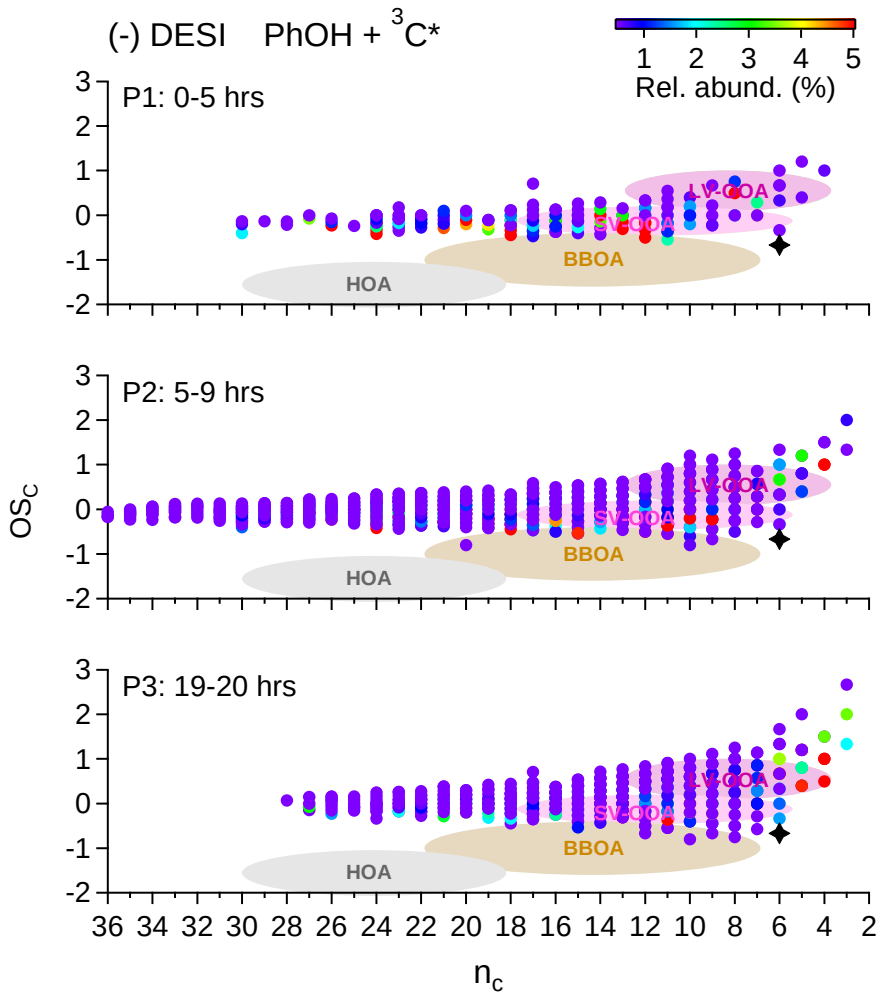

Figure S6. OS_C and n_C of PhOH aqSOA formed during different stages of $^3C^*$-mediated reactions determined based on (-) nano-DESI MS spectra. Signals are colored by the relative abundance of the molecules. The black star at $n_C = 6$ represents PhOH. The shaded ovals indicate locations of different ambient organic aerosol classes reported in Kroll et al. (*2011*).

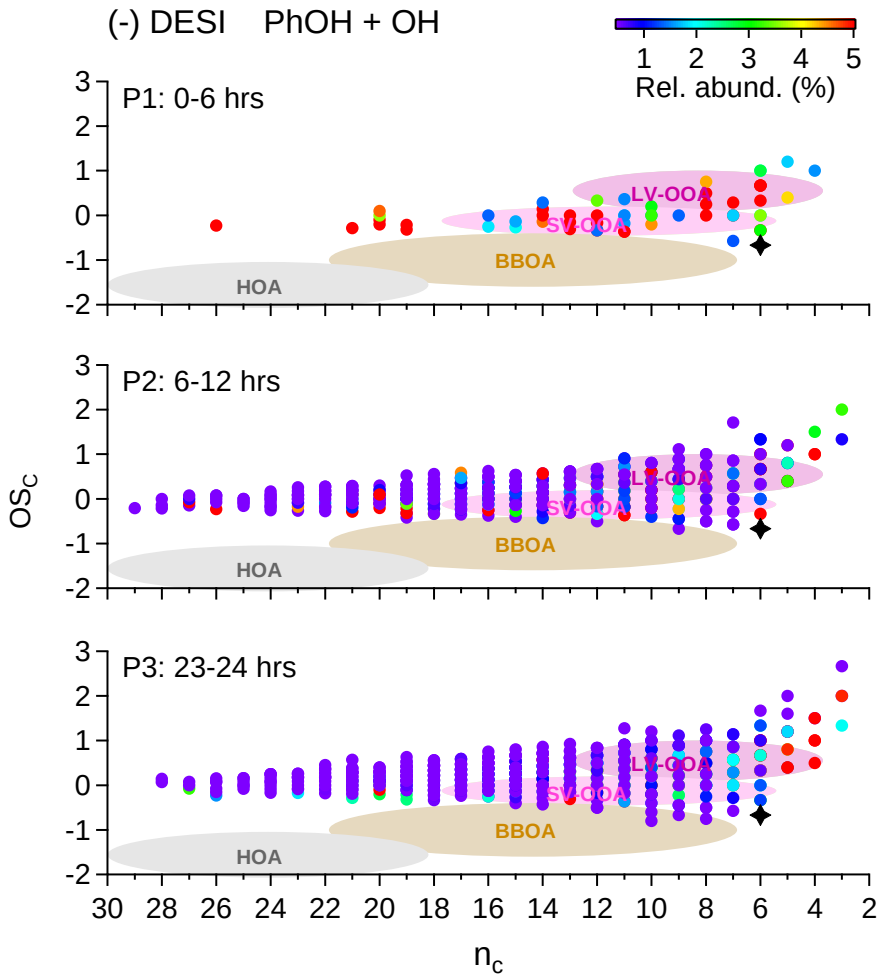

Figure S7. OS_C and n_C of PhOH aqSOA formed during different stages of •OH-mediated reactions determined based on (-) nano-DESI MS spectra. Signals are colored by the relative abundance of the molecules. The black star at $n_C = 6$ represents PhOH. The shaded ovals indicate locations of different ambient organic aerosol classes reported in Kroll et al. (*2011*).

References

Aiken, A. C., Decarlo, P. F., Kroll, J. H., Worsnop, D. R., Huffman, J. A., Docherty, K. S., Ulbrich, I. M., Mohr, C., Kimmel, J. R., Sueper, D., Sun, Y., Zhang, Q., Trimborn, A., Northway, M., Ziemann, P. J., Canagaratna, M. R., Onasch, T. B., Alfarra, M. R., Prevot, A. S. H., Dommen, J., Duplissy, J., Metzger, A., Baltensperger, U., and Jimenez, J. L.: O/c and om/oc ratios of primary, secondary, and ambient organic aerosols with high-resolution time-of-flight aerosol mass spectrometry, Environ. Sci. Technol., 42, 4478-4485, 10.1021/es703009q, 2008.

Allan, J. D., Delia, A. E., Coe, H., Bower, K. N., Alfarra, M. R., Jimenez, J. L., Middlebrook, A. M., Drewnick, F., Onasch, T. B., Canagaratna, M. R., Jayne, J. T., and Worsnop, D. R.: A generalised method for the extraction of chemically resolved mass spectra from aerodyne aerosol mass spectrometer data, J. Aerosol Sci., 35, 909-922, 10.1016/j.jaerosci.2004.02.007, 2004.

Canagaratna, M. R., Jayne, J. T., Jimenez, J. L., Allan, J. D., Alfarra, M. R., Zhang, Q., Onasch, T. B., Drewnick, F., Coe, H., Middlebrook, A., Delia, A., Williams, L. R., Trimborn, A. M., Northway, M. J., DeCarlo, P. F., Kolb, C. E., Davidovits, P., and Worsnop, D. R.: Chemical and microphysical characterization of ambient aerosols with the aerodyne aerosol mass spectrometer, Mass Spectrom. Rev., 26, 185-222, 10.1002/mas.20115, 2007.

DeCarlo, P. F., Kimmel, J. R., Trimborn, A., Northway, M. J., Jayne, J. T., Aiken, A. C., Gonin, M., Fuhrer, K., Horvath, T., Docherty, K. S., Worsnop, D. R., and Jimenez, J. L.: Field-deployable, high-resolution, time-of-flight aerosol mass spectrometer, Anal. Chem., 78, 8281-8289, 10.1021/ac061249n, 2006.

Jaitly, N., Mayampurath, A., Littlefield, K., Adkins, J. N., Anderson, G. A., and Smith, R. D.: Decon2ls: An open-source software package for automated processing and visualization of high resolution mass spectrometry data, BMC Bioinformatics, 10, 87, 10.1186/1471-2105-10-87, 2009.

Kroll, J. H., Donahue, N. M., Jimenez, J. L., Kessler, S. H., Canagaratna, M. R., Wilson, K. R., Altieri, K. E., Mazzoleni, L. R., Wozniak, A. S., Bluhm, H., Mysak, E. R., Smith, J. D., Kolb, C. E., and Worsnop, D. R.: Carbon oxidation state as a metric for describing the chemistry of atmospheric organic aerosol, Nat. Chem., 3, 133-139, 10.1038/nchem.948, 2011.

Roach, P. J., Laskin, J., and Laskin, A.: Nanospray desorption electrospray ionization: An ambient method for liquid-extraction surface sampling in mass spectrometry, Analyst, 135, 2233-2236, 10.1039/c0an00312c, 2010.

Roach, P. J., Laskin, J., and Laskin, A.: Higher-order mass defect analysis for mass spectra of complex organic mixtures, Anal. Chem., 83, 4924-4929, 10.1021/ac200654j, 2011.